https://dx.doi.org/10.22161/ijaers.76.40 ISSN: 2349-6495(P) | 2456-1908(O)

Damage Identification of Vehicle Brake Disks by the use of Impedance-Based SHM and Unsupervised Machine Learning Method

Stanley Washington Ferreira de Rezende, Bruno Pereira Barella, Jose dos Reis Vieira de Moura Jr

Department of Mathematics and Technology, IMTec, Federal University of Goias, Catalao-GO, Brazil

***Abstract*— *Although SHM (Structural Health Monitoring) has been widely used for aeronautical purposes, in the last decades new application scenarios have become applicable, such as the civil and automotive industries. Automotive components are increasing the maximum operational efficiency, aiming to obtain greater performance and safety of its mechanical systems at low production and maintenance costs. In this context, it is necessary to make predictive studies related to the incipient damages or about the useful life of the structures. The brake system represents one of the most important mechanical systems in a passenger vehicle since it deals directly with the preservation of their lives. Thus, in this contribution a regular vehicle brake disc is studied in order to evaluate the sensitivity of the impedance-based SHM application to identify mechanical changes and propose a method to check their integrities. With the purpose to promote structural changes, a virtual damage was created by mass addition with small magnets attached on the surface of the disc in different positions. Further, some experiments were conducted to have several state conditions of the brake discs (pristine and several virtually damaged cases). Then, the unsupervised machine learning technique called K-Means Clustering Method was applied to the data set and a quadratic regression model was used as well based on RMSD damage metric of the cases. Obtained results show the applicability of the method in the identification of damages, as well as the potential of the use of unsupervised machine learning methods and mathematical models in the context of SHM.*

Keywords*— *Electromechanical Impedance-based SHM, Unsupervised Machine Learning, K-Means Clustering Analysis, Structural Health Monitoring, Vehicle Brake Disk.

I. INTRODUCTION

The main purpose of the SHM (Structural Health Monitoring) is to implement a predictive maintenance system to use the mechanical component along of its useful life, minimizing costs and reducing stoppages [13, 14, 19-21]. One of the most important mechanical systems in a regular passenger vehicle is the brake system composed by brake pads and brake disc. This system was designed to promote wear in brake pads which are exchanged periodically while the brake discs continues to has a longer useful life. Thus, this investigation was considered because the importance of the brake system in a vehicle and the preventive maintenance aspect of the component.

The impedance-based SHM is applied today and under investigation for a several applications in aeronautical studies [4, 7, 8]. However, with the advances of new manufacturing lines and low-cost electronic circuits, the technique becomes to be applicable for other maintenance purposes of lower order of costs [10, 17, 20].

It has been shown that the electrical impedance from the piezoelectric ceramic (sensor/actuator) surface bonded to a structure can be directly associated with the mechanical impedance of the structure to which it is bonded. By using the same piezoelectric element as a sensor/actuator, a simple testing device, containing a smaller number of components and cables has been developed [16].

[11] first proposed the impedance method as a technique for structural monitoring. The technique was later improved by [1-3, 5, 6, 9, 12, 13, 15, 18, 20, 21]. It has been shown that electromechanical impedance (EMI) techniques utilize the two modes of behavior of the piezoelectric material. When stressed mechanically, an electric charge is produced, which is called the Direct Piezoelectric Effect. Conversely, when an electric field is

https://dx.doi.org/10.22161/ijaers.76.40 *ISSN: 2349-6495(P) | 2456-1908(O)*

applied in the poling direction, the piezoelectric patch undergoes mechanical deformation and this is known as the Inverse Piezoelectric Effect. Fig. 1 shows a one-dimensional electromechanical model of the impedance-based structural health monitoring system.

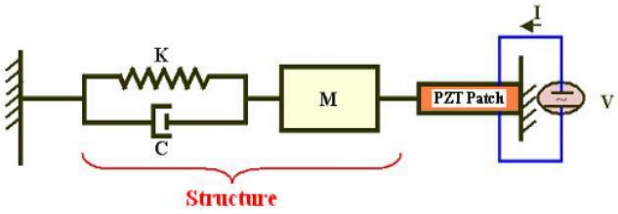

Fig. 1: One-dimensional electromechanical model.

The PZT patch (Lead Zirconate Titanate) is considered as a thin bar undergoing axial vibrations in response to the alternating voltage applied by the impedance analyzer. Equation (1) shows the expression for the electromechanical admittance [11].

$$Y(\omega) = \frac{I}{V} = i\omega a\left(\bar{\varepsilon}_{33}^{T}(1 - i\delta) - \frac{z(\omega)}{z(\omega)+Z_a(\omega)} d_{3x}^{2} \hat{Y}_{xx}^{E}\right) \quad (1)$$

where V is the voltage applied to the PZT patch, I is the output current, a is the geometric constant of the PZT patch, d_{3x} is the piezoelectric coupling constant in the arbitrary x direction at zero stress, $\hat{Y}_{xx}^{E}$ is the Young's modulus and $\bar{\varepsilon}_{33}^{T}$ is the complex dielectric constant at zero stress, ω is the angular frequency, Z_a and Z are the PZT's and the structure's complex mechanical impedance, respectively, and δ is the dielectric loss tangent of the PZT patch. This equation states that the electrical impedance of the PZT patch bonded onto the structure is directly related to the mechanical impedance of the structure [5-8, 11, 12, 14, 21]. Consequently, since the mechanical impedance of the PZT patch is assumed to be constant, any change in the electrical admittance is expected to be equal to the change in the mechanical impedance of the structure.

The method uses frequencies usually higher than 30kHz that are applied to the PZT patch that is bonded to the surface of the structure to evaluate the signal modifications as captured by the sensor. The PZT patches use a low voltage (< 1V) and generate high frequency excitation at given points in the structure [16]. However, the voltage equal to 1V leads to satisfactory results with respect to the identification of structural changes.

Basically, the technique consists in obtaining the frequency response functions (FRFs) of the structure in order to further compare the modification in these signals as caused by damage. A modification in the FRFs would indicate the presence of damage.

The impedance-based SHM measures the real part of the impedance signature by the use of piezoelectric sensor/actuator bonded in the investigated structure. Then, both baseline (pristine condition) and damaged signatures are compared in order to calculate the severity of the problem as well as locate it [12-14, 21]. This quantitative comparison in this work uses the RMSD (Root Mean Squared Deviation) damage metric to do evaluations [12, 14]. This damage metric was proposed by [19], being expressed according to (2):

$$RMSD = \sum_{i=1}^{n} \sqrt{\frac{\left(R_i^B - R_i^D\right)^2}{\left(R_i^B\right)^2}} \quad (2)$$

where R_i^B and R_i^D is, respectively, the real part of the impedance signature from baseline and damaged conditions and n is the size of the sample set [12, 14, 21].

II. EXPERIMENTAL PROCEDURE

The proposed experimental procedure used one regular vehicle brake disc with dimensions of 100x260x260 mm. Then, two simulated damage conditions were proposed by addition of mass in places where real wearing occurs, i.e., the area of the wear use to occurs. For this damage tests were used magnets (10x10x10 mm) and Fig. 2 illustrates the test positions, which the damage #2 is closer to the PZT patch.

Damage #1

Damage #2

Fig. 2: Brake disc with the PZT patch and damages (added masses).

https://dx.doi.org/10.22161/ijaers.76.40 *ISSN: 2349-6495(P) | 2456-1908(O)*

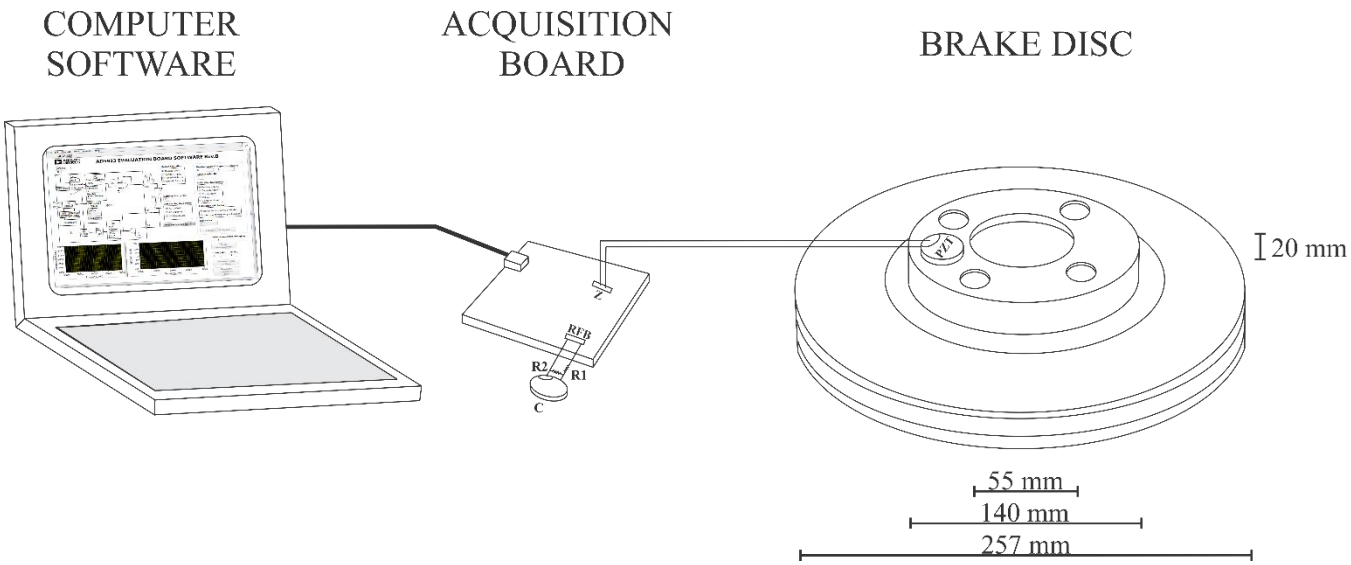

Fig. 3: Experimental setup for the data gathering.

The used experimental setup to gather the data samples is illustrated by the Fig. 3. The system is composed by on vehicle brake disc (structure to be investigated), one data acquisition card (analogic-digital converter) and a laptop with the software interface for data gathering.

The impedance-based SHM measures the signature in high frequencies because on these ranges it is possible to check small damages or cracks. In this proposed work the frequency range obtained by trial and error was 20.5-28.17 kHz.

The data acquisition system used in this contribution was an EVAL AD5933-EBZ card from Analog Devices and one circular PZT patch (diameter of 20 mm and thickness of 3 mm) was used as sensor/actuator. For each condition test was gathered 10 samples obtaining a total of 30 samples (10 baseline, 10 damage #1 and 10 damage #2). Fig. 4 illustrates the data acquisition system (EVAL AD5933-EBZ) used in the experiment.

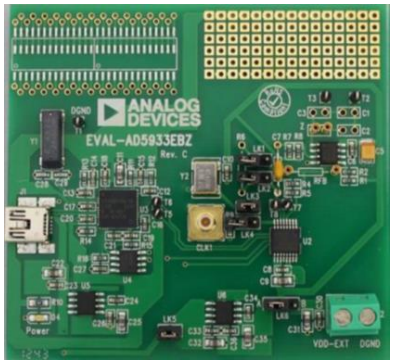

Fig. 4: Evaluation board EVAL-AD5933EBZ.

The card communicates to the computer by USB port and uses the software called "AD5933 Evaluation Board Software Rev.B" supplied by the manufacturer Analog Devices for gathering purposes. Although the measured impedance is important to define the status of the structure, this information needs to be processed and classified before by filtering and metric calculations.

III. RESULTS AND DISCUSSION

The evaluated frequency range was 20.5-28.17 kHz in a step of 15 Hz, presenting a total of 511 points. According to the references, it was considered only the real part of the impedance signatures due to the mechanical properties are associated with them. All experiments were conducted and the impedance signatures were compared for each condition and it was possible to check amplitude as well as frequency peak deviations as illustrated by Fig. 5.

Fig. 5 illustrates the real part of the impedance signature and it is evident how hard can be the process of evaluation from the direct impedance curve. In addition, due to the presence of an insignificant deviation between the signatures an assertive quantitative analysis of the presence of damage is also not possible since only a qualitative analysis could be performed in the signatures.

Moreover, another factor of great impact in the decision process of the presence of damages is the extension of the data sets necessary to carry out such analyzes, since the computational cost to scan large volumes of data is often not accessible, thus necessitating a process of intermediate abstraction previously to the quantitative analysis of these.

https://dx.doi.org/10.22161/ijaers.76.40 *ISSN: 2349-6495(P) | 2456-1908(O)*

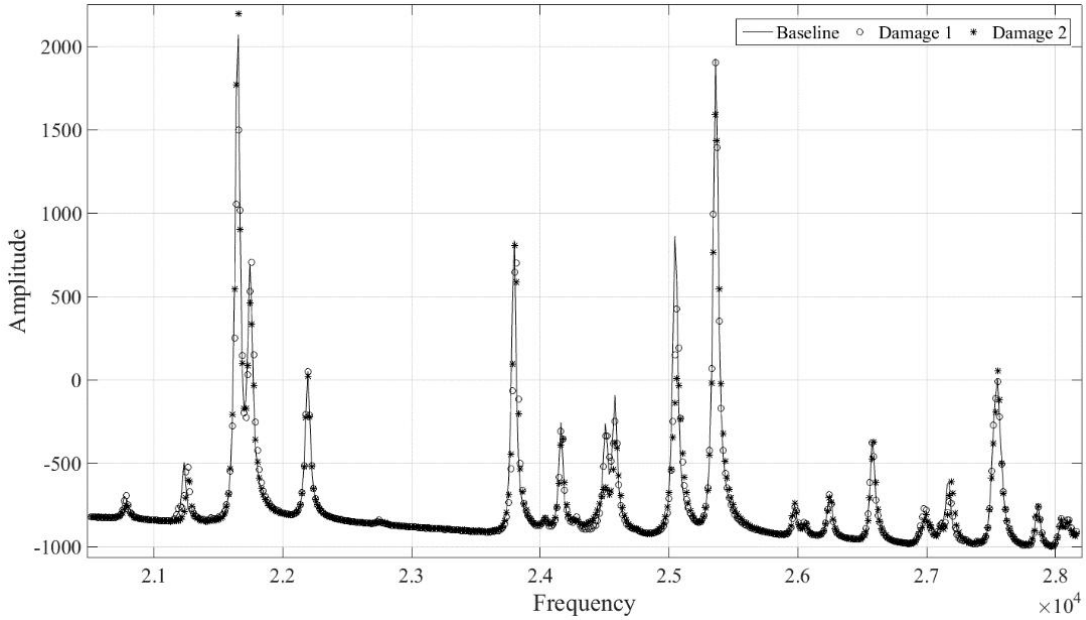

Fig. 5: Baseline and damage signatures – real part of the impedance.

Thus, in order to delimit a subset of signal abstractions, whose information contained are consistent and at the same time representative of the different groups of signals, the *k*-means clustering algorithm was applied to the set of samples that were later splitted into 5 subgroups, in which each observation of the signal was grouped according to its proximity to the average of each of the cluster of the group to which it belonged. Table 1 shows the different subsets obtained by the *k*-means method in relation to the respective clusters.

Table 1: Subsets of data obtained through the k-means algorithm for each sample of each level in relation to their respective clusters. The data represent the frequency clusters of each sample.

Cluster – 1			
Sample	**Baseline**	**Damage #1**	**Damage #2**
1	-126,3718	-169,2348	-138,8865
2	-126,3581	-169,2329	-138,9159
3	-126,3992	-169,2055	-138,8474
4	-126,4853	-169,1331	-138,8513
5	-126,3249	-169,1625	-138,7886
6	-126,1819	-169,1135	-138,7436
7	-126,2505	-169,0607	-138,7202
8	-126,1096	-169,0509	-138,7397
9	-125,9022	-169,0451	-138,7515
10	-126,1703	-169,0998	-138,7710

Cluster – 2			
Sample	**Baseline**	**Damage #1**	**Damage #2**
1	-150,8963	-175,9178	-126,3581
2	-150,9002	-175,9452	-126,3992
3	-150,7260	-175,9413	-126,4853
4	-150,8865	-175,9491	-126,3249
5	-150,8493	-175,8160	-126,1820
6	-150,8728	-175,8904	-126,2505
7	-150,8063	-175,8415	-126,1096
8	-150,7691	-175,7867	-125,9022
9	-150,7906	-175,7436	-126,1703
10	-150,7554	-175,7730	-126,7886

Cluster – 3			
Sample	**Baseline**	**Damage #1**	**Damage #2**
1	-169,2329	-138,9159	-150,9002
2	-169,2055	-138,8474	-150,7260
3	-169,1331	-138,8513	-150,8865
4	-169,1624	-138,7886	-150,8493
5	-169,1135	-138,7436	-150,8728
6	-169,0607	-138,7202	-150,8063
7	-169,0509	-138,7397	-150,7691
8	-169,0450	-138,7515	-150,7906
9	-169,0998	-138,7710	-150,7554
10	-168,7906	-142,1135	-148,7886

Cluster – 4			
Sample	**Baseline**	**Damage #1**	**Damage #2**
1	-175,9452	-126,3992	-169,2055
2	-175,9413	-126,4853	-169,1331
3	-175,9491	-126,3249	-169,1624
4	-175,8160	-126,1820	-169,1135
5	-175,8904	-126,2505	-169,0607
6	-175,8415	-126,1096	-169,0509
7	-175,7867	-125,9022	-169,0450
8	-175,7436	-126,1703	-169,0998
9	-175,7730	-126,7886	-168,7906
10	-175,2035	-126,7045	-168,7534

Cluster – 5			
Sample	**Baseline**	**Damage #1**	**Damage #2**
1	-138,8474	-150,7260	-175,9413
2	-138,8513	-150,8865	-175,9491

https://dx.doi.org/10.22161/ijaers.76.40 *ISSN: 2349-6495(P) | 2456-1908(O)*

3	-138,7886	-150,8493	-175,8160
4	-138,7436	-150,8728	-175,8904
5	-138,7202	-150,8063	-175,8415
6	-138,7397	-150,7691	-175,7867
7	-138,7515	-150,7906	-175,7436
8	-138,7710	-150,7554	-175,7730
9	-142,1135	-148,7886	-175,2035
10	-141,8102	-149,0391	-175,2172

From Table 1 we can identify that the applicability of the *k*-means method allowed an optimization of the computational cost due to the reduction of the dimensionality of the data set. Abstracting each sample of signal, formed by 511 points, to a vector of 5 points of frequency amplitude, without lack of relevant information to the decision process.

Subsequently in order to transform this evaluation in a quantitative result, it was used the RMSD Damage Metric for the cluster set obtained from de *k*-means method which were splitted into groups by boxplot chart, obtaining the Fig. 6. Thus, the boxplot is responsible to check the independence of the damage groups and then propose a parameter to represent this variation.

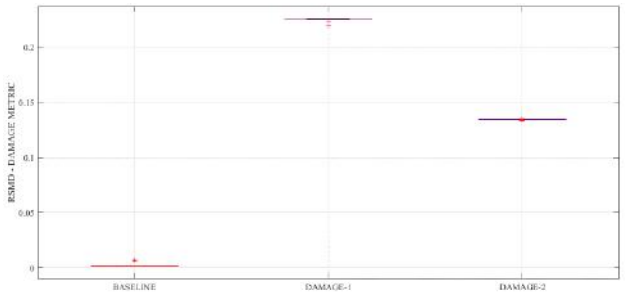

Fig. 6: Damage metric Boxplots for each cluster set of each condition test.

According to the Fig. 6, the proposed methodology was able to detect damage (statistically split) as well as locate it, showing its applicability of the impedance-based SHM for the proposed work. Also, it is possible to understand by the boxplot that the closer the damage is, the greater is the RMSD damage metric severity. Then, based on this observation it was proposed the modeling of the damage case by the use of such damage metrics by a regression model.

Considering 30 samples (10 for each group), it was selected randomly 8 samples from each case to build a regression model classifying the damage case based on the RMSD damage metric, obtained after clustering. Then, it was checked the model by the use of the missing data amount (2 for each group).

Table 2 illustrates all RMSD damage metrics of clusters obtained from the 30 samples.

Table 2: All RMSD damage metrics obtained for the 10 repetitions of the 3 damage groups.

Baseline	Damage #1	Damage #2
0,0016	0,2248	0,1345
0,0016	0,2248	0,1348
0,0018	0,2251	0,1342
0,0018	0,2255	0,1346
0,0018	0,2252	0,1347
0,0018	0,2256	0,1346
0,0017	0,2260	0,1347
0,0017	0,2253	0,1350
0,0070	0,2232	0,1338
0,0065	0,2193	0,1358

From Table 2 it was selected 2 columns of samples (gray rows) for each group to be removed and the Fig. 7 illustrates the correspondent type of damage regression model built.

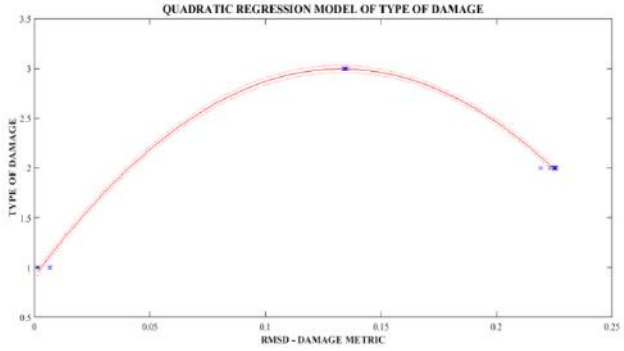

Fig. 7: Type of damage quadratic regression model.

Fig. 7 illustrates the same aspect of the boxplot. However, now it is possible to determine a type of damage with a degree of precision (about 99.7%), corresponding to the correlation of the data amount. This value is not very precise because the model includes only three conditions: baseline, damage #1 and damage #2 and these RMSD damage metrics are not quite linear (baseline, for example is completely different from damage #1). For a best quadratic regression model, it is necessary to build a model with a linear increase of the RMSD damage metrics for previously studied positions of damage, not made randomly like this preliminary study.

After the calculation of the regression model, it is necessary to validate the model in order to check the mathematical expression for new values not used to create the model as represented in Fig. 8.

For this purpose, to check the model, it was used the missed figures (gray rows) from Table 1. Then, it was predicted the type of damage from these 2 samples for each 3 groups by the use of the correspondent RMSD damage metrics and the quadratic regression model obtained.

https://dx.doi.org/10.22161/ijaers.76.40 *ISSN: 2349-6495(P) | 2456-1908(O)*

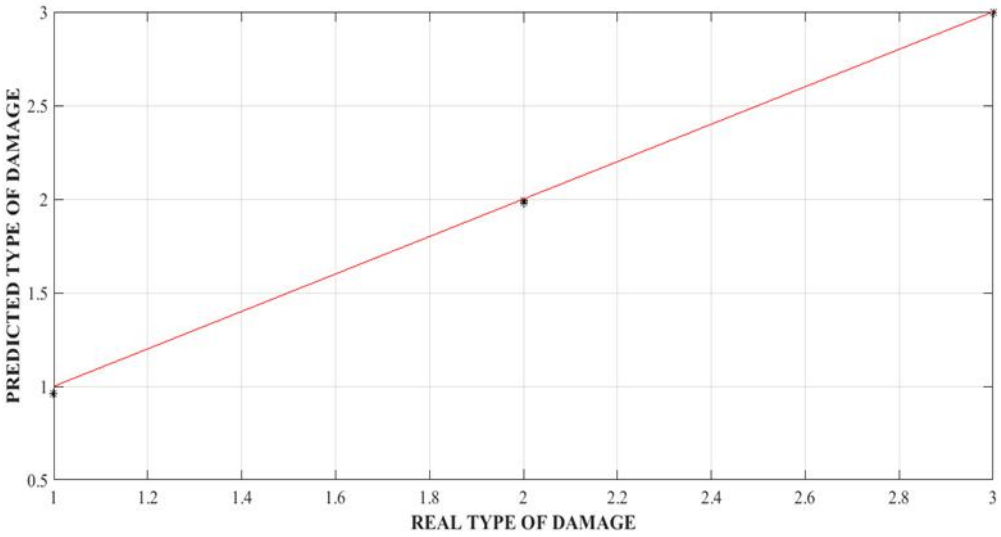

Fig. 8: Validation of the type of damage regression model.

Fig. 8 represents the checking procedure of the type of damage regression model. This chart plots in the x-axis the real type of damage of the missed figures from Table 2. In y-axis is plotted the figures of the same missed cases calculated by the use of the type of damage regression model (Fig. 7).

The correlation between both types of damages (real versus calculated by the regression model) shows also a correlation about 99.7%, indicating a validation of the type of damage regression model obtained previously.

IV. CONCLUSIONS

This contribution proposes a new approach to investigate mechanical changes in brake discs by the use of impedance-based SHM in a quantitative aspect. For this, the *k*-means algorithm, an unsupervised machine learning technique was applied in order to reduce the dimensionality of the data without loss of relevant information in the decision process.

During the quantitative analysis, the boxplot obtained from the experiments illustrates a very good separation between different damage conditions allowing the calculation of a regression model for an automated way to investigate the type of damage based on the RMSD damage metric. Although preliminary results obtained are not straightly applied, they show a potential of use of the technique for this kind of problems. Concluding, these nondestructive tests associated to the machine learning technique shows the ability to detect incipient damages in brake systems helping in the future to improve the safety of automotive components.

ACKNOWLEDGEMENTS

S. W. F. R. and B. P. B. thanks to CAPES for his grant scholarship.

REFERENCES

[1] Allen, D. W., Peairs, D. M. and Inman, D. J. (2004). Damage detection by applying statistical methods to PZT impedance measurements. In: *Smart Structures and Materials 2004: Smart Structures and Integrated Systems (Vol. 5390, pp. 513-520). International Society for Optics and Photonics*.

[2] Chaudhry, Z. A., Joseph, T., Sun, F. P. and Rogers, C. A. (1995). Local-area health monitoring of aircraft via piezoelectric actuator/sensor patches. In: *Smart Structures and Materials 1995: Smart Structures and Integrated Systems (Vol. 2443, pp. 268-276). International Society for Optics and Photonics*.

[3] Chaudhry, Z., Lalande, F., Ganino, A., Rogers, C. and Chung, J. (1995). Monitoring the integrity of composite patch structural repair via piezoelectric actuators/sensors. In: *36th Structures, structural dynamics and materials conference* (p. 1074).

[4] Franco, V. R. (2009). Monitoramento da integridade em estruturas aeronáuticas. (Master Thesis), Paulista State University, Faculty of Engineering of Ilha Solteira.

[5] Giurgiutiu, V. and Zagrai, A. N. (2000). Characterization of piezoelectric wafer active sensors. *Journal of Intelligent Material Systems and Structures*, 11(12), 959-976.

[6] Giurgiutiu, V., Zagrai, A. and Jing Bao, J. (2002). Piezoelectric wafer embedded active sensors for aging aircraft structural health monitoring. *Structural Health Monitoring*, 1(1), 41-61.

[7] Giurgiutiu, V., Redmond, J. M., Roach, D. P. and Rackow, K. (2000). Active sensors for health monitoring of aging aerospace structures. In: *Smart Structures and Materials 2000: Smart Structures and Integrated Systems (Vol. 3985, pp. 294-305). International Society for Optics and Photonics*.

[8] Giurgiutiu, V. and Zagrai, A. (2005). Damage detection in thin plates and aerospace structures with the electro-mechanical impedance method. *Structural Health Monitoring*, 4(2), 99-118.

https://dx.doi.org/10.22161/ijaers.76.40 *ISSN: 2349-6495(P) | 2456-1908(O)*

[9] Hu, X., Zhu, H. and Wang, D. (2014). A study of concrete slab damage detection based on the electromechanical impedance method. *Sensors*, 14(10), 19897-19909.

[10] Kobayashi, M., Wu, K. T., Song, L., Jen, C. K. and Ad, N. (2009). Structural health monitoring of composites using integrated and flexible piezoelectric ultrasonic transducers. *Journal of intelligent material systems and structures*, 20(8), 969-977.

[11] Liang, C., Sun, F. P. and Rogers, C. A. (1997). Coupled electro-mechanical analysis of adaptive material systems-determination of the actuator power consumption and system energy transfer. *Journal of intelligent material systems and structures*, 8(4), 335-343.

[12] Moura Jr, J. D. R. V. and Steffen Jr, V. (2004). Impedance-based health monitoring: frequency band evaluation. In: *Proceedings of the 22nd International Modal Analysis Conference (IMAC XXII), Detroit, Michigan, USA* (No. 901).

[13] Moura Jr, J. D. R. V. and Steffen Jr, V. (2006). Impedance-based health monitoring for aeronautic structures using statistical meta-modeling. *Journal of intelligent material systems and structures*, 17(11), 1023-1036.

[14] Palomino, L. V. (2008). Análise das métricas de dano associadas à técnica da impedância eletromecânica para o monitoramento de integridade estrutural. (Master Thesis), Federal University of Uberlândia, Uberlândia.

[15] Park, G., Kabeya, K., Cudney, H. H. and Inman, D. J. (1999). Impedance-based structural health monitoring for temperature varying applications. *JSME International Journal Series A Solid Mechanics and Material Engineering*, 42(2), 249-258.

[16] Park, G., Sohn, H., Farrar, C. R. and Inman, D. J. (2003). Overview of piezoelectric impedance-based health monitoring and path forward. *Shock and vibration digest*, 35(6), 451-464.

[17] Silva, R. N. F., Tsuruta, K. M., Neto, R. F. and Steffen Jr, V. (2016). The use of electromechanical impedance based structural health monitoring technique in concrete structures. In: *Proceedings of the 8th European Workshop on Structural Health Monitoring, Bilbao, Spain* (pp. 5-8).

[18] Soh, C. K., Tseng, K. K., Bhalla, S. and Gupta, A. (2000). Performance of smart piezoceramic patches in health monitoring of a RC bridge. *Smart materials and Structures*, 9(4), 533.

[19] Sun, F. P., Chaudhry, Z., Liang, C. and Rogers, C. A. (1995). Truss structure integrity identification using PZT sensor-actuator. *Journal of Intelligent material systems and structures*, 6(1), 134-139.

[20] Talakokula, V., Bhalla, S. and Gupta, A. (2018). Monitoring early hydration of reinforced concrete structures using structural parameters identified by piezo sensors via electromechanical impedance technique. *Mechanical Systems and Signal Processing*, 99, 129-141.

[21] Tsuruta, K. M., Rabelo, D. S., Guimarães, C. G., Cavalini Jr, A. A., Neto, R. F. and Steffen Jr, V. (2017). Electromechanical impedance-based fault detection in a rotating machine by using an operating condition compensation approach. In: *A Tribute Conference Honoring Daniel Inman (Vol. 10172, p. 1017206). International Society for Optics and Photonics*.